

PERTURBATION-BASED ERROR ANALYSIS OF ITERATIVE IMAGE RECONSTRUCTION ALGORITHM FOR X-RAY COMPUTED TOMOGRAPHY

Jung Kuk Kim, Jeffrey A. Fessler, Zhengya Zhang

EECS Department, University of Michigan, Ann Arbor, MI 48109-2122, USA

ABSTRACT

Statistical iterative image reconstruction methods are compute intensive. Fixed-point calculations can substantially reduce the computational load, but also increase quantization error. To investigate the effect of fixed-point quantization, we analyze the error propagation after introducing perturbation in a diagonally preconditioned gradient descent algorithm for X-ray computed tomography. The effects of the quantization error in forward-projection, back-projection, and image update are calculated using the open loop and loop gain of the iterative algorithm. We derive an analytical upper bound on the quantization error variance of the reconstructed image and show that the quantization step size can be chosen to meet a given upper bound. The analytical results are confirmed by numerical simulations.

I. INTRODUCTION

Statistical iterative image reconstruction methods for X-ray computed tomography (CT) have been proposed to improve image quality and reduce dose [1]. These methods are based on accurate projection models and measurement statistics, and formulated as maximum likelihood (ML) estimation [2]. Iterative algorithms have been designed to estimate the image by minimizing a cost function [3]–[5].

CT image reconstruction algorithms are usually implemented in 32-bit single-precision floating-point quantization to provide high image quality. Fixed-point (integer) arithmetic uses much less hardware resources than floating-point and can shorten the latency [6], but it introduces quantization errors and potentially degrades the image quality. Therefore it is desirable to analyze the quantization effects to assess the feasibility of a fixed-point conversion.

In this paper, we model the effect of fixed-point quantization as a perturbation of floating-point arithmetic by injecting uniform white noise after the arithmetic [7]. For simplicity of the analysis, we choose a diagonally preconditioned gradient descent algorithm with a quadratic regularizer [8], and inject noise in the three steps of an iterative image reconstruction: forward-projection, back-projection, and image update. We derive an upper bound on the quantization error variance

This work was supported in part by a Korea Foundation for Advanced Studies (KFAS) Scholarship and the University of Michigan. J. A. Fessler's effort is supported by NIH grant R01-HL-098686.

of the image update in every iteration and the results are verified by numerical simulations based on a $40 \times 40 \times 4$ test object over 90 projection views.

II. BACKGROUND

A CT system captures a large series of projections at different view angles, recorded as sinogram. Mathematically, sinogram y can be modeled as $y = Af + \epsilon$, where f represents the volume being imaged and A is the system matrix, or the forward-projection model, and ϵ denotes measurement noise. The goal of image reconstruction is to estimate the 3D image f from the measured sinogram y . A statistical image reconstruction method estimates f , or \hat{f} , based on measurement statistics, which can be formulated as a weighted least square (WLS) problem [2].

$$\hat{f} = \arg \min_f \frac{1}{2} \|y - Af\|_W^2, \quad (1)$$

where W is a diagonal matrix with entries based on photon measurement statistics [2]. To control undesired noise in \hat{f} of (1), a penalty term is added to form a penalized weighted least square (PWLS) [2], [8] cost function:

$$\hat{f} = \arg \min_f \Psi(f) = \arg \min_f \frac{1}{2} \|y - Af\|_W^2 + \beta R(f), \quad (2)$$

where $R(f)$ is known as the regularizer and β is a regularization parameter. For simplicity of analysis, we choose a quadratic regularizer that adds to the cost function the square of differences among neighboring pixels, or $R(f) = \|Cf\|^2/2$, where C is the difference matrix.

Using a quadratic regularizer and assuming that $(A'WA + \beta C'C)$ is invertible, the solution to (2) is given by $\hat{f} = (A'WA + \beta C'C)^{-1} A'Wy$. However, the practical size of matrix A for a commercial axial CT scanner is 10 million by 10 million [2], thus evaluating the inverse of $A'WA + \beta C'C$ is inefficient, if not infeasible. Alternatively, iterative methods have been proposed [3]–[5]. In this paper we consider a diagonally preconditioned gradient descent method to solve (2) [5], [8]:

$$\begin{aligned} \hat{f}^{(i+1)} &= \hat{f}^{(i)} - D \nabla \Psi(\hat{f}^{(i)}) \\ &= \hat{f}^{(i)} + D \left[A'W(y - A\hat{f}^{(i)}) - \beta C'C \hat{f}^{(i)} \right]. \end{aligned} \quad (3)$$

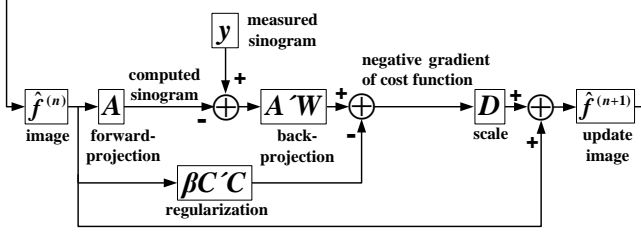


Fig. 1. Block diagram of iterative image reconstruction.

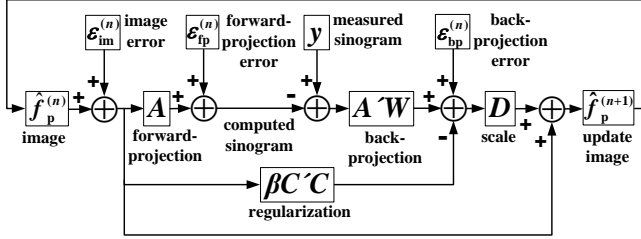


Fig. 2. Iterative image reconstruction with perturbed forward-projection, back-projection and image update.

Fig. 1 shows a block diagram of this iterative image reconstruction method. Typically a FBP reconstructed image is used as the initial image, $\hat{f}^{(0)}$. In each iteration, a new 3D image estimate $\hat{f}^{(i+1)}$ is obtained by updating the previous image $\hat{f}^{(i)}$ with a step of the negative gradient of the cost function $\Psi(\hat{f})$ scaled by a diagonal matrix D . This algorithm is guaranteed to converge to the unique minimizer of Ψ when D is chosen properly [5]. This is a one subset version of the ordered subsets (OS) algorithm given in [5].

III. PERTURBATION-BASED ERROR ANALYSIS

We analyze the effect of perturbation in iterative image reconstruction and show that both the maximum and the mean error variance in an image update are bounded for a given level of uniform white noise. Hereafter, we define $\hat{f}_p^{(n)}$ as the n^{th} image update of the perturbed iterative algorithm, and $e^{(n)}$ as the corresponding image error relative to the unperturbed version $\hat{f}^{(n)}$, i.e., $e^{(n)} = \hat{f}^{(n)} - \hat{f}_p^{(n)}$.

III-A. Perturbation of forward-projection

We proceed by first perturbing the forward-projection to model the effect of fixed-point quantization [7]. We add a random error vector, $\varepsilon_{\text{fp}}^{(n)}$, to the ideal forward-projection, as illustrated in Fig. 2. We further assume that the error samples are uncorrelated. Specifically, we assume

$$\begin{aligned} \varepsilon_{\text{fp}}^{(n)} &\sim U \left[-\frac{\Delta_{\text{fp}}}{2}, \frac{\Delta_{\text{fp}}}{2} \right], \quad \text{cov}(\varepsilon_{\text{fp}}^{(i)}, \varepsilon_{\text{fp}}^{(i)}) = \frac{\Delta_{\text{fp}}^2}{12} I, \\ \text{cov}(\varepsilon_{\text{fp}}^{(i)}, \varepsilon_{\text{fp}}^{(j)}) &= 0 \quad \forall i, \forall j, i \neq j, \end{aligned} \quad (4)$$

where Δ_{fp} denotes the quantization step size.

From (3), the first image update of the perturbed algorithm can be written as

$$\begin{aligned} \hat{f}_p^{(1)} &= \hat{f}^{(0)} + D \left[A'W \left(y - \left(A\hat{f}^{(0)} + \varepsilon_{\text{fp}}^{(0)} \right) \right) - \beta C'C \hat{f}^{(0)} \right] \\ &= \hat{f}^{(1)} + K_{\text{fp}} \varepsilon_{\text{fp}}^{(0)}, \end{aligned} \quad (5)$$

where $K_{\text{fp}} \triangleq -DA'W$ is the open loop gain of the error due to perturbation in forward-projection. Similarly, we have the second image update as

$$\hat{f}_p^{(2)} = \hat{f}_p^{(1)} + D \left[A'W \left(y - \left(A\hat{f}_p^{(1)} + \varepsilon_{\text{fp}}^{(1)} \right) \right) - \beta C'C \hat{f}_p^{(1)} \right]. \quad (6)$$

Substituting (5) into (6) and simplification yields

$$\hat{f}_p^{(2)} = \hat{f}^{(2)} + MK_{\text{fp}} \varepsilon_{\text{fp}}^{(0)} + K_{\text{fp}} \varepsilon_{\text{fp}}^{(1)},$$

where $M \triangleq I - D(A'WA + \beta C'C)$ is the loop gain of the error in this iterative method. (Note that M is related to the Hessian of the cost function [8], which is given by $H = A'WA + \beta C'C$). By induction, the image update of the n^{th} iteration and the image update error are given by

$$\begin{aligned} \hat{f}_p^{(n)} &= \hat{f}^{(n)} + e^{(n)} \\ e^{(n)} &= \sum_{k=0}^{n-1} M^k K_{\text{fp}} \varepsilon_{\text{fp}}^{(n-1-k)}. \end{aligned}$$

Using (4), the mean of $e^{(n)}$ is zero, and the covariance is

$$\text{cov}(e^{(n)}, e^{(n)}) = \frac{\Delta_{\text{fp}}^2}{12} \sum_{k=0}^{n-1} M^k K_{\text{fp}} K_{\text{fp}}' (M^k)'. \quad (7)$$

Note that a covariance matrix is positive semidefinite [9], and its eigenvalues are nonnegative [10]. Thus, an upper bound on the error variance is the maximum eigenvalue, i.e., spectral radius, of the covariance matrix of $e^{(n)}$. Evaluating the spectral radius is nontrivial due to the term M^k . Since matrix D is a real diagonal matrix with positive diagonal entries, we can decompose M as

$$M = I - DH = D^{\frac{1}{2}} \left(I - D^{\frac{1}{2}} H D^{\frac{1}{2}} \right) D^{-\frac{1}{2}}.$$

The Hessian matrix H is a nonnegative definite and so is $I - D^{\frac{1}{2}} H D^{\frac{1}{2}}$, by the design of D . Thus by the spectral theorem [11], there exists a unitary matrix U and a diagonal matrix Σ such that $I - D^{\frac{1}{2}} H D^{\frac{1}{2}} = U \Sigma U'$. Then M becomes

$$M = D^{\frac{1}{2}} U \Sigma U' D^{-\frac{1}{2}}. \quad (8)$$

Similarly, $(A'W)(A'W)'$ is also nonnegative definite and can be decomposed using a unitary matrix V and a nonnegative diagonal matrix F [11]. It follows that

$$K_{\text{fp}} K_{\text{fp}}' = (-DA'W)(-DA'W)' = D(VFV')D. \quad (9)$$

Substituting (8) and (9) into (7), we have

$$\begin{aligned} & \text{cov} \left(e^{(n)}, e^{(n)} \right) \\ &= \frac{\Delta_{\text{fp}}^2}{12} \sum_{k=0}^{n-1} D^{\frac{1}{2}} U \Sigma^k U' D^{\frac{1}{2}} (V F V') D^{\frac{1}{2}} U \Sigma^k U' D^{\frac{1}{2}}. \end{aligned}$$

Thus the spectral radius equals the 2-norm and its upper bound can be derived using the matrix norm property that $\|AB\| \leq \|A\| \|B\|$ [12]. After considerable simplification, we have

$$\begin{aligned} & \rho \left(\text{cov} \left(e^{(n)}, e^{(n)} \right) \right) \\ &= \max_{x: \|x\|=1} \left(x' \text{cov} \left(e^{(n)}, e^{(n)} \right) x \right) \\ &= \frac{\Delta_{\text{fp}}^2}{12} \max_{x: \|x\|=1} \left(\sum_{k=0}^{n-1} \| F^{\frac{1}{2}} V' D^{\frac{1}{2}} U \Sigma^k U' D^{\frac{1}{2}} x \|^2 \right) \\ &\leq \frac{\Delta_{\text{fp}}^2}{12} \rho(F) \rho(D^2) \frac{1 - \rho(\Sigma^2)^n}{1 - \rho(\Sigma^2)}. \end{aligned} \quad (10)$$

The spectral radius of the covariance matrix measures the maximum error variance in the n^{th} iteration. i.e., $\sigma_{(n)\text{max}}^2 \triangleq \rho(\text{cov}(e^{(n)}, e^{(n)}))$. Next, we analyze the mean error variance in an image update, which is related to the trace, or sum of diagonal entries, of the covariance matrix, i.e., $\sigma_{(n)\text{mean}}^2 \triangleq \text{tr}(\text{cov}(e^{(n)}, e^{(n)})) / n_v$, where n_v is the number of diagonal entries in the covariance matrix. Using the property that $\text{tr}(AB) \leq \rho(B)\text{tr}(A)$ [11], we have

$$\begin{aligned} & \text{tr} \left(\text{cov} \left(e^{(n)}, e^{(n)} \right) \right) \\ &= \frac{\Delta_{\text{fp}}^2}{12} \text{tr} \left(\sum_{k=0}^{n-1} D^{\frac{1}{2}} U \Sigma^k U' D^{\frac{1}{2}} (V F V') D^{\frac{1}{2}} U \Sigma^k U' D^{\frac{1}{2}} \right) \\ &\leq \frac{\Delta_{\text{fp}}^2}{12} \sum_{k=0}^{n-1} \rho(\Sigma^k) \text{tr} \left(D^{\frac{1}{2}} (V F V') D^{\frac{1}{2}} U \Sigma^k U' D \right) \\ &\leq \frac{\Delta_{\text{fp}}^2}{12} \text{tr}(D(V F V') D) \frac{1 - \rho(\Sigma^2)^n}{1 - \rho(\Sigma^2)}. \end{aligned} \quad (11)$$

To guarantee the convergence of iterative reconstruction algorithm, the matrix D is always selected such that $D^{-1} \succ H$, i.e., $D^{-1} - H$ is positive definite, which implies $\rho(I - DH) < 1$, where H is the Hessian of the cost function [8]. It follows that

$$\begin{aligned} \rho(\Sigma) &= \rho(U'(I - D^{\frac{1}{2}} H D^{\frac{1}{2}})U) = \rho(I - D^{\frac{1}{2}} H D^{\frac{1}{2}}) \\ &= \rho(D^{-\frac{1}{2}}(I - DH)D^{\frac{1}{2}}) = \rho(I - DH) < 1. \end{aligned}$$

In steady state as $n \rightarrow \infty$, the upper bounds of (10) and (11) become

$$\begin{aligned} \sigma_{(n)\text{max}}^2 &\leq \rho(\text{cov}(e^{(\infty)}, e^{(\infty)})) \leq \frac{\Delta_{\text{fp}}^2}{12} \frac{\rho(D^2)\rho(F)}{1 - \rho(\Sigma^2)}, \\ \sigma_{(n)\text{mean}}^2 n_v &\leq \text{tr}(\text{cov}(e^{(\infty)}, e^{(\infty)})) \leq \frac{\Delta_{\text{fp}}^2}{12} \frac{\text{tr}(D(V F V') D)}{1 - \rho(\Sigma^2)}. \end{aligned}$$

Therefore, both the maximum and the mean error variance of an image update are bounded. For example, given $\epsilon > 0$, if we choose Δ_{fp} such that

$$\Delta_{\text{fp}} < \sqrt{\frac{12(1 - \rho(\Sigma^2)^2)}{\rho(D^2)}} \sqrt{\frac{1}{\rho(F)}} \sqrt{\epsilon},$$

then

$$\sigma_{(\infty)\text{max}}^2 < \epsilon, \quad \sigma_{(\infty)\text{mean}}^2 < \epsilon.$$

The result implies that we can make the error due to perturbation in forward-projection arbitrarily small for this algorithm by choosing an appropriate quantization step size, provided quantization noise can be modeled as in (4).

III-B. Perturbation of forward-projection, back-projection, and image update

Following the derivation from the previous section, we can also model the effect of fixed-point quantization in the back-projection and image update by injecting uniform white noises $\varepsilon_{\text{bp}}^{(n)}$ and $\varepsilon_{\text{im}}^{(n)}$, as indicated in Fig. 2. Similar to (4), we make the following assumptions:

$$\varepsilon_{\text{bp}}^{(n)} \sim U \left[-\frac{\Delta_{\text{bp}}}{2}, \frac{\Delta_{\text{bp}}}{2} \right], \quad \varepsilon_{\text{im}}^{(n)} \sim U \left[-\frac{\Delta_{\text{im}}}{2}, \frac{\Delta_{\text{im}}}{2} \right], \quad (12)$$

where Δ_{bp} and Δ_{im} denote the quantization step sizes of back-projection and image update respectively.

Similar to (5), we can express the perturbed image update of the first iteration as

$$\begin{aligned} \hat{f}_{\text{p}}^{(1)} &= (\hat{f}^{(0)} + \varepsilon_{\text{im}}^{(0)}) + D[A'W(y - (A(\hat{f}^{(0)} + \varepsilon_{\text{im}}^{(0)}) + \varepsilon_{\text{fp}}^{(0)})) \\ &\quad + \varepsilon_{\text{bp}}^{(0)} - \beta C' C(\hat{f}^{(0)} + \varepsilon_{\text{im}}^{(0)})] \\ &= \hat{f}^{(1)} + K_{\text{fp}} \varepsilon_{\text{fp}}^{(0)} + K_{\text{bp}} \varepsilon_{\text{bp}}^{(0)} + M \varepsilon_{\text{im}}^{(0)}, \end{aligned}$$

where $K_{\text{bp}} \triangleq D$ is the open loop gain of the error due to perturbation in back-projection. It follows that the image update error in the n^{th} iteration is

$$e^{(n)} = \sum_{k=0}^{n-1} (M^k (K_{\text{fp}} \varepsilon_{\text{fp}}^{(n-1-k)} + K_{\text{bp}} \varepsilon_{\text{bp}}^{(n-1-k)} + M \varepsilon_{\text{im}}^{(n-1-k)})).$$

We assume independence of the three noise vectors. Using (4), (8), (9), and (12), the mean of $e^{(n)}$ is zero, and the covariance can be written as

$$\begin{aligned} \text{cov} \left(e^{(n)}, e^{(n)} \right) &= \frac{\Delta_{\text{fp}}^2}{12} \sum_{k=0}^{n-1} (M^k K_{\text{fp}} K_{\text{fp}}' (M^k)') + \\ &\frac{\Delta_{\text{bp}}^2}{12} \sum_{k=0}^{n-1} (M^k K_{\text{bp}} K_{\text{bp}}' (M^k)') + \frac{\Delta_{\text{im}}^2}{12} \sum_{k=0}^{n-1} (M^{k+1} (M^{k+1})'). \end{aligned}$$

Following a similar approach as in the previous section, we can derive the upper bounds on the spectral radius and

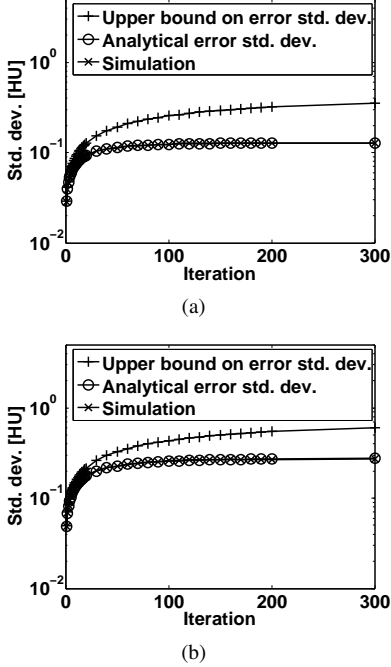


Fig. 3. Theoretical bound and numerical simulation of standard deviation of the image updates : (a) forward-projection with the quantization step size of $\Delta_{fp} = 2^7$ [HU×mm] (b) forward-projection, back-projection, and image update with $\Delta_{fp} = 2^7$ [HU×mm], $\Delta_{bp} = 2^{15}$ [mm], $\Delta_{im} = 2^{-3}$ [HU].

the trace of the covariance matrix.

$$\begin{aligned} \rho(\text{cov}(e^{(\infty)}, e^{(\infty)})) &\leq \frac{\Delta_{fp}^2 \rho(D^2)\rho(F)}{12(1-\rho(\Sigma^2))} + \frac{\Delta_{bp}^2 \rho(D^2)}{12(1-\rho(\Sigma^2))} \\ &\quad + \frac{\Delta_{im}^2 \rho(\Sigma^2)\rho(D)\rho(D^{-1})}{12(1-\rho(\Sigma^2))}, \\ \text{tr}(\text{cov}(e^{(\infty)}, e^{(\infty)})) &\leq \frac{\Delta_{fp}^2 \text{tr}(VFV'D^2)}{12(1-\rho(\Sigma^2))} + \frac{\Delta_{bp}^2 \text{tr}(D^2)}{12(1-\rho(\Sigma^2))} \\ &\quad + \frac{\Delta_{im}^2 \rho(\Sigma^2)\text{tr}(I)}{12(1-\rho(\Sigma^2))}. \end{aligned}$$

Therefore, both the maximum and the mean error variance of the reconstructed image are bounded after considering perturbation in forward-projection, back-projection, and image update. The error can be made arbitrarily small for this algorithm by choosing an appropriate quantization step size.

IV. RESULTS AND CONCLUSION

To verify the analysis, we performed numerical simulations of an iterative reconstruction of a $40 \times 40 \times 4$ test object in an axial cone-beam arc-detector X-ray CT system with a detector size of 170×10 over 90 projection views. The PWLS diagonally preconditioned gradient descent algorithm (3) was simulated with a quadratic roughness regularizer. We evaluated analytical quantization error variance and its upper bound in each iteration, which are compared to measured quantization error variance from simulations by

injecting uniformly distributed error vectors that correspond to quantization step sizes of $\Delta_{fp} = 2^7$ [HU×mm], $\Delta_{bp} = 2^{15}$ [mm], and $\Delta_{im} = 2^{-3}$ [HU]. Fig. 3 shows the standard deviation of the image update error due to (a) perturbation in forward-projection alone and (b) perturbation in forward-projection, back-projection, and image update. The measured standard deviation matches the analytical standard deviation and stays below the upper bound. Due to limited space, we only show one set of quantization step size, but alternative choices could be equally used. Both the analytical and simulation results in Fig. 3 point to the conclusion that the error variance of image updates converges to a fixed level after a sufficient number of iterations. Note that evaluating the analytical error variance is not feasible for large object sizes. Quantizing iterative methods to confirm our perturbation model and tightening the upper bound remain our future work.

V. REFERENCES

- [1] J. A. Fessler, “Statistical image reconstruction methods for transmission tomography,” *Handbook of Medical Imaging, Volume 2. Medical Image Processing and Analysis*, pp. 1–70, 2000.
- [2] T. M. Buzug, *Computed tomography from photon statistics to modern cone-beam CT*. New York: Springer-Verlag, 2009.
- [3] S. Kawata and O. Nalcioglu, “Constrained iterative reconstruction by the Conjugate Gradient method,” *IEEE Trans. Med. Imag.*, vol. 4, pp. 65–71, 1985.
- [4] Z. Q. Luo and P. Tseng, “On the convergence of the coordinate descent method for convex differentiable minimization,” *J. Optim. Theory Appl.*, vol. 72, no. 1, pp. 7–35, 1992.
- [5] H. Erdogan and J. A. Fessler, “Ordered subsets algorithms for transmission tomography,” *Phys. Med. Biol.*, vol. 44, pp. 2835–51, 1999.
- [6] J. Kim, Z. Zhang, and J. A. Fessler, “Hardware acceleration of iterative image reconstruction for X-ray computed tomography,” in *IEEE Conf. Acoust. Speech Sig. Proc.*, May 2011, pp. 1697–1700.
- [7] A. V. Oppenheim, R. W. Schaffer, and J. R. Buck, *Discrete-time signal processing*. New Jersey: Prentice Hall, 1997.
- [8] J. A. Fessler, *Image reconstruction: Algorithms and analysis*. Book in preparation.
- [9] J. A. Gubner, *Probability and random processes for electrical and computer engineers*. Cambridge University Press, 2006.
- [10] D. C. Lay, *Linear algebra and its applications*. Pearson Education, Inc, 2003.
- [11] K. Hoffman and R. Kunze, *Linear Algebra*. New Jersey: Prentice Hall, 2003.
- [12] L. N. Trefethen and D. Bau, *Numerical linear algebra*. SIAM, 1997.